Proceedings World Geothermal Congress 2015
Melbourne, Australia, 19-25 April 2015

A Thermal-Hydraulic-Mechanical Fully Coupled Model for Heat Extraction in Enhanced Geothermal Systems

Wenjiong Cao, Wenbo Huang, Fangming Jiang*

Laboratory of Advanced Energy Systems, Guangzhou Institute of Energy Conversion, Chinese Academy of Sciences (CAS), Guangzhou 510640, China

jiangfm@ms.giec.ac.cn

Keywords: THM coupling; local thermal non-equilibrium; thermal-pore-elastic; EGS

ABSTRACT

During the heat extraction in enhanced geothermal systems (EGS), the porosity and permeability of the heat reservoir can be greatly affected by the multi-physical coupling of Thermal (T), Hydraulic (H), and Mechanical (M) processes. In the present work we develop a three-dimensional transient model fully coupling the subsurface THM behaviors during EGS heat extraction process. The local thermal non-equilibrium is assumed when describing the heat exchange between the rock matrix and heat transmission fluid, and the variable properties of the fluid are combined to realize the bi-directional coupling of thermal and hydraulic behaviors. The thermal-pore-elastic model is adopted to calculate the effective stress of the rock matrix and further to derive the local porosity and permeability. Case study with respect to an imaginary EGS demonstrates the validity and capability of the developed model. Results indicate that the model can be used for heat extraction simulation of more practical EGSs.

1. INTRODUCTION

Simulating the heat extraction process and predicting how much heat can be extracted from an enhanced geothermal system (EGS) reservoir are relatively involved tasks and thus remain still as major challenges for the geothermal industry (MIT Report, 2006). To address such challenges it is desirable to develop reliable numerical models dealing with the inter-coupled Thermal– Hydraulic–Mechanical (THM) processes in EGS subsurface reservoir. Koh et al. (2011) mentioned that circulating cold fluid into the reservoir can lead to large amounts of stress energy release inside the rock matrix. How does EGS performance including its production temperature, mass flow rate of circulation fluid, lifetime, and heat extraction ratio etc. relate the THM coupling behaviors? This can be unraveled or better understood via numerical modeling.

During the past decades, considerable efforts have been expended in the THM model development and numerical studies relevant to EGS heat extraction. Rutqvist (2002, 2011)and Jeanne et al. (2014) reviewed the developed models of hydromechanical coupling in an aquifer and summarized a number of well-known empirical approaches for estimations of normal stress across fractured medium. Ghassemi and Zhou (2011), Ghassemi et al. (2007), and Rawal and Ghassemi (2014) numerically investigated the poroelastic and thermoelastic responses of a reservoir or fractures in a reservoir upon the injection of cold water. McDermott et al. (2005, 2006) studied the influence of THM coupling on the heat extraction from reservoir in crystalline rocks with an experimentally validated geomechanical model developed by themselves. The results indicated that changes of fracture aperture and closure were caused by changes of normal stress acting on fractures, which was the dominant mechanism for thermal stress inducing changes of reservoir permeability. The physical properties of the injected fluid, such as density, viscosity and heat capacity are speculated to play a significant role in the fluid-rock interactions. Nevertheless, to the best of our knowledge, there are no published THM numerical models that have fully coupled the effects of variable fluid properties.

In the present work, we present a three-dimensional transient model fully coupling the subsurface THM behaviors during EGS heat extraction process. The local thermal non-equilibrium assumption is adopted to describe the heat transport in the reservoir, and variable fluid properties are considered to realize the bi-directional coupling of thermal and hydraulic behaviors. A thermal-pore-elastic model is employed to calculate the effective stress of the rock matrix and further to derive the local porosity and permeability. A case study with respect to an imaginary EGS will be performed to demonstrate the validity and capability of the developed model.

2. THM COUPLING MODEL FOR EGS HEAT EXTRACTION

2.1 Model equations

We focus on the heat extraction from EGS subsurface reservoir and consider an imaginary EGS consisting of an injection well, a production well or multiple production wells, an artificial heat reservoir, and rocks enclosing the reservoir as described in our previous publications(Jiang et al., 2013). The reservoir is taken as an equivalent porous medium with uniform porosity ε and permeability K. Model equations describing the heat transport and fluid flow are listed below.

Fluid continuity equation:

$$\frac{\partial(\varepsilon\rho_{\mathrm{f}})}{\partial t}+\nabla\cdot(\rho_{\mathrm{f}}\mathbf{u})=0 \tag{1}$$

Fluid momentum equation:

$$\frac{\partial(\rho_{\mathrm{f}}\mathbf{u})}{\partial t}+\frac{\rho_{\mathrm{f}}\mathbf{u}}{\varepsilon}\nabla\mathbf{u}=-\nabla p+\nabla\cdot\mu\nabla\mathbf{u}-\frac{\mu}{K}\mathbf{u}+\varepsilon\rho_{\mathrm{f}}\mathbf{g} \tag{2}$$

Energy conservation in solid rock or rock matrix in the porous reservoir:

$$\frac{\partial[(1-\varepsilon)\rho_{\mathrm{s}}c_{ps}T_{\mathrm{s}}]}{\partial t}=\nabla\cdot(\lambda_{\mathrm{s}}^{\mathrm{eff}}\nabla T_{\mathrm{s}})-ha(T_{\mathrm{s}}-T_{\mathrm{f}}) \tag{3}$$

Energy conservation in fluid:

$$\frac{\partial[\varepsilon\rho_{\mathrm{f}}c_{pf}T_{\mathrm{f}}]}{\partial t}+\nabla\cdot(\mathbf{u}\rho_{\mathrm{f}}c_{pf}T)=\nabla\cdot(\lambda_{\mathrm{f}}^{\mathrm{eff}}\nabla T_{\mathrm{f}})+ha(T_{\mathrm{s}}-T_{\mathrm{f}}) \tag{4}$$

where $\mathbf{u}$, p, T_{f} and T_{s} are the primary variables to be solved, denoting the superficial fluid velocity vector, fluid pressure, fluid temperature, and rock temperature, respectively; ρ_{f}, ρ_{s} are the density of the fluid and solid rock, respectively; c_{pf}, c_{ps} are the specific heat capacity of the fluid and solid rock, respectively; λ_{f}, λ_{s} are the heat conductivity of the fluid and solid rock, respectively; h denotes the convective heat transfer coefficient between rock matrix and fluid in the reservoir, and a the specific surface area of fractures. The last terms of Eq. 3 and Eq. 4, $\pm ha(T_{\mathrm{s}}\text{-}T_{\mathrm{f}})$ describe the heat exchange between rock matrix and fluid in the reservoir; the negative sign of this term in Eq. 3 means the heat is extracted from the rock and the positive sign of this term in Eq. 4 means the heat is absorbed by the working fluid. The fluid properties in the above equations including ρ_{f}, μ, c_{pf} and λ_{f} are considered to be dependent on the fluid pressure and temperature, which will be detailed in Section 2.2. We have implemented the so-called single-domain treatment (Jiang et al., 2013) to the model geometry: $\varepsilon=0$ and $K=0$ in the solid rock region, $\varepsilon=1$ and $K=\infty$ in the injection and production wells, ε and K both have finite values in the porous reservoir. With this single-domain treatment we can unify the mathematical description (Eqs. (1) and (2)) to fluid flow in different regions and computationally we simplify the treatment of interfaces between regions. The effective heat conductivity in the porous region is implemented, which is the intrinsic heat conductivity timed by the volume fraction raised to power of 1.5.

The mechanics stress field in the rock is described by the following mean total stress equation (Hu et al., 2013):

$$\frac{3(1-\upsilon)}{(1+\upsilon)}\nabla^2\sigma_m=\frac{2\alpha(1-2\upsilon)}{(1+\upsilon)}\nabla^2 p+\frac{6\beta B(1-2\upsilon)}{(1+\upsilon)}\nabla^2 T-\nabla\cdot\boldsymbol{F} \tag{5}$$

where, σ_m denotes the mean total stress, υ is the Poisson's ratio of rock, α the Biot's coefficient, β the linear thermal expansion coefficient, and B the bulk module of the rock. The three terms on the right side of Eq. (5) describe the effects of the poreelastic stress, the thermalelastic stress and the external body force, respectively.

2.2 Thermophysical properties of water

We adopt the International Association for the Properties of Water and Steam (IAPWS, 2007) model to establish the variable properties of water. The model consists of a set of equations for different phase of water. Under EGS subsurface conditions, the water is normally in liquid phase. We have

$$\frac{g(p,T)}{R_wT}=\gamma(\pi,\tau)=\sum_{i=1}^{34}n_i(7.1-\pi)^{I_i}(\tau-1.222)^{J_i} \tag{6}$$

where $g(p,T)$ is the Gibbs free energy; R_{w} is the mass-specific gas constant of water, R_{w}=461.526 J/(kg•K); $\gamma(\pi,\tau)$, π and τ denote the dimensionless forms of the specific Gibbs free energy, pressure and temperature, respectively ($\pi = p/p^*$ and $\tau = T^*/T$, with p^*=16.53 MPa and T^*= 1386 K). Values of the coefficients n_i and exponents I_i and J_i in Eq. (5) can be referred to IAPWS (2007). The density and specific heat are calculated from the partial differentials of $\gamma(\pi,\tau)$, as

$$\rho_{\mathrm{w}}(p,T)=\frac{p}{R_wT\pi(\partial\gamma/\partial\pi)} \tag{7}$$

$$c_{p\mathrm{w}}(p,T)=-R_w\tau^2(\partial^2\gamma/\partial\tau^2) \tag{8}$$

The heat conductivity and viscosity of water are calculated by the following equations (IAPWS, 2011, 2008):

$$\lambda_{\mathrm{w}}(T,\rho)=\lambda^*\times\bar{\lambda}_0(\bar{T})\times\bar{\lambda}_1(\bar{T},\bar{\rho})+\bar{\lambda}_2(\bar{T},\bar{\rho}) \tag{9}$$

$$\mu_{\mathrm{w}}(T,\rho)=\mu^*\times\bar{\mu}_0(\bar{T})\times\bar{\mu}_1(\bar{T},\bar{\rho})\times\bar{\mu}_2(\bar{T},\bar{\rho}) \tag{10}$$

where the reference values $\lambda^*=1.0\times10^{-3}$ W/(m•K), $\mu^*=1.0\times10^{-6}$ Pa•s; $\bar{T}$ and $\bar{\rho}$ denote the dimensionless forms of the temperature and density, respectively ($\bar{T}=T/T'$ and $\bar{\rho}=\rho/\rho'$, with $T'=647.096$ K and $\rho'=322.0$ kg/m^3); the terms with

subscript 0, 1 and 2 are the dilute gas term, finite density term and critical enhancement term, respectively. The dilute gas term and the finite density term of the heat conductivity and viscosity are given by:

$$\bar{\lambda}_0(\bar{T}) = \frac{\sqrt{\bar{T}}}{\sum_{i=0}^{4} \frac{L_i}{\bar{T}^i}} \tag{11}$$

$$\bar{\mu}_0(\bar{T}) = \frac{100\sqrt{\bar{T}}}{\sum_{i=0}^{3} \frac{H_i}{\bar{T}^i}} \tag{12}$$

$$\bar{\lambda}_1(\bar{T},\bar{\rho}) = \exp\left[\bar{\rho}\sum_{i=0}^{4}\left(\left(\frac{1}{\bar{T}}-1\right)^i \sum_{j=0}^{5} L_{ij}\left(\bar{\rho}-1\right)^j\right)\right] \tag{13}$$

$$\bar{\mu}_1(\bar{T},\bar{\rho}) = \exp\left[\bar{\rho}\sum_{i=0}^{5}\left(\left(\frac{1}{\bar{T}}-1\right)^i \sum_{j=0}^{6} H_{ij}\left(\bar{\rho}-1\right)^j\right)\right] \tag{14}$$

where L_i , L_{ij} , H_i and H_{ij} are all constant and their values can be referred to IAPWS (2011, 2008). Since only the liquid phase of water is considered in this work, the critical enhancement terms of the heat conductivity and viscosity are omitted, i.e. $\bar{\lambda}_2(\bar{T},\bar{\rho}) = 0$ and $\bar{\mu}_2(\bar{T},\bar{\rho}) = 1$.

2.3 THM Coupling

The THM processes during EGS heat extraction are inter-coupled. The fluid flow results in convective heat transport. Temperature- and pressure- dependent thermophysical properties of fluid further complete the inter-coupling between thermal and hydraulic processes. The fluid pressure and temperature induce stress changes in the rock or rock matrix. The mechanical process in the rock or rock matrix affects the TH processes as the porosity and permeability in the reservoir are related to the stress field in the rock or rock matrix. In terms of the mean total stress calculated from Eq. (5), local porosity and permeability in the reservoir are updated with the following equations (Hu et al., 2013. Rutqvist et al., 2002):

$$\sigma' = \sigma_m - \alpha p \tag{15}$$

$$\varepsilon = \varepsilon_r + (\varepsilon_0 - \varepsilon_r)\mathrm{e}^{-\xi\sigma'} \tag{16}$$

$$K = K_0 \mathrm{e}^{\zeta(\varepsilon/\varepsilon_0 - 1)} \tag{17}$$

where the subscripts *0* and *r* denote the parameter values under zero effective stress and a high effective stress, respectively; α is the Biot's coefficient as in Eq. (5); the exponentials ξ and ζ are both constants. In this work, we take α=1.0, ξ=5.0×10^8 1/Pa, ζ=22.2.

3. CASE STUDY

The geometry of an imaginary quintuplet EGS considered in the present work is schematically shown in Fig. 1. The artificial heat reservoir is a 500m×500m×500m cubic volume. The injection and production well boreholes penetrate the reservoir and all have 0.2m×0.2m squared cross-section in the xy-plane. Due to the geometrical symmetry, only a quarter of the geometry is simulated.

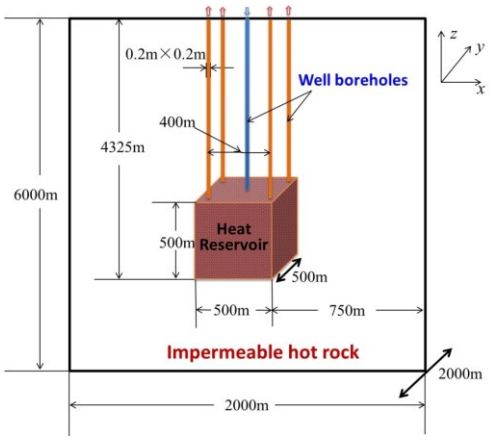

Fig.1: Geometry and dimensions of the quintuplet EGS considered.

Mesh system and initial temperature distribution are displayed in Fig.2. The mesh system totally has around 200,000 numerical elements. Initial temperature of the rock is assumed to increase linearly against the depth direction (-z) with a gradient of 4K per 100m and a ground temperature of 300K. Initially, the temperature of working fluid is assumed to be locally the same as that of the rock. During heat extraction, cold fluid with temperature of 343K is injected into the heat reservoir under a prescribed 10MPa pressure difference between the injection well inlet and the production well outlet. The pressure at the center of the heat reservoir is assigned a constant pressure, 40MPa. Values of other parameters considered in the case study are summarized in Table 1.

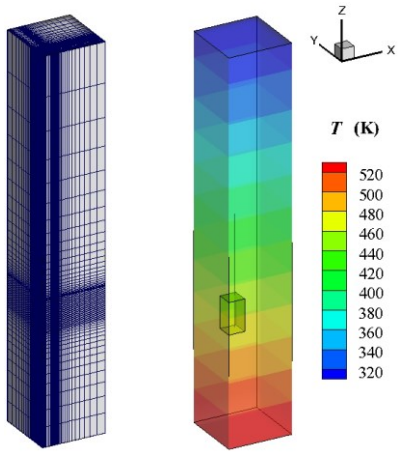

Fig.2: Mesh system and initial rock temperature.

Table 1: Model parameters

Parameter	**Value**
Rock density, ρ_s (kg/m^3)	2650.0
Rock heat capacity, c_{ps} (J/kg/K)	1000.0
Rock thermal conductivity, λ_s (W/m/K)	2.4
Rock Poisson's ratio, υ	0.2
Rock bulk modulus, K (GPa)	9.3
Rock linear thermal expansion, β	1.15×10^{-6}
Biot's coefficient, α	1.0
Initial porosity, ε	0.01
Initial permeability, K (m^2)	1.0×10^{-14}
Fluid properties	Eq.(7-10)

The equation group consisting of Eqs. (1)-(5) together with the above-described boundary conditions and initial conditions are solved in the commercial CFD (computational fluid dynamics) flow solver, Fluent®, which is based on the finite volume approximation. By customizing the flexible User Defined Functions (UDF) available in Fluent®, non-standard scalar transport equations and various source terms, geo-physical properties, and non-standard advection-convective terms in the governing equations are implemented. The well-known SIMPLE (Semi-Implicit Method for Pressure Linked Equation) algorithm is used to address the pressure-velocity coupling. The first order upwind differencing scheme is generally used for discretization of the spatial-derivative terms and a fully implicit scheme for discretization of the transient terms. To accelerate convergence, the AMG (algebraic multi-grid) iterative method is applied to solve the linearized algebraic equations.

Evolution of rock temperature in the reservoir is displayed in Fig. 3. As cold fluid is injected into the reservoir, a low temperature region is formed about the injection well. This low temperature region gradually expands toward the production well with the proceeding of the EGS operation.

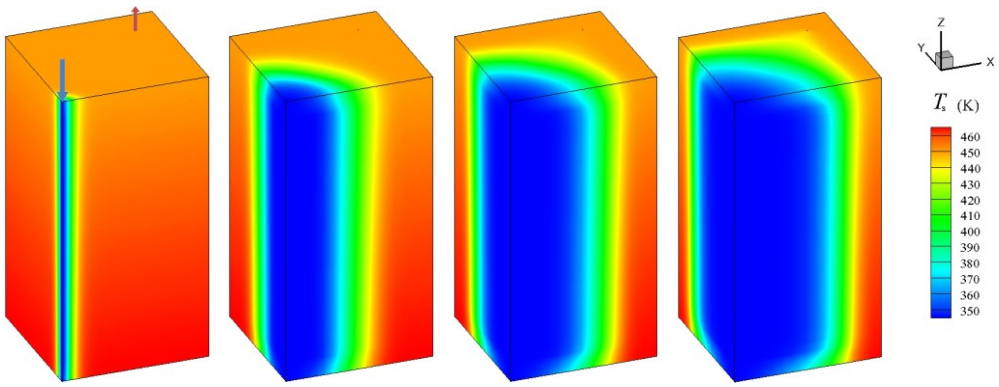

(a) 1 year **(b) 5 years** **(c) 10 years** **(d) 15 years**

Fig. 3: Rock temperature distribution in the heat reservoir

Evolution of pore pressure in the reservoir is shown in Fig. 4. The pore pressure remains high only in a very limited region about the injection well borehole, indicating most of the flow resistance is originated from the fluid flow in this region.

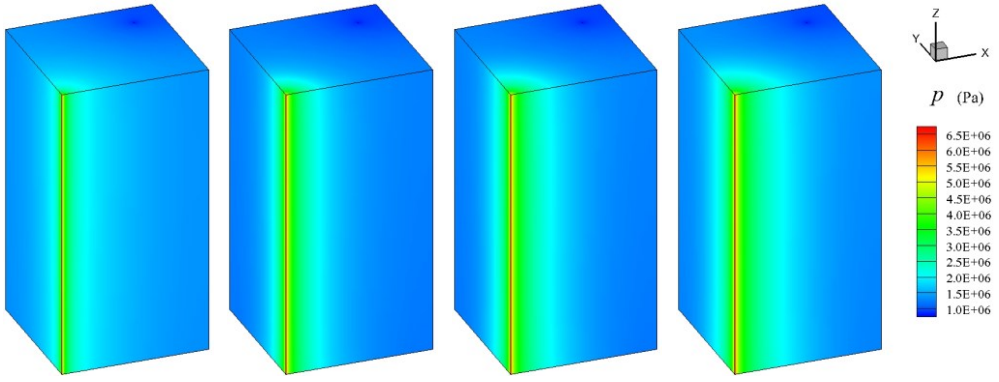

(a) 1 year **(b) 5 years** **(c) 10 years** **(d) 15 years**

Fig. 4: Pore pressure distribution in the heat reservoir

Fig. 5 shows the evolution of the mean total stress in the rock matrix. There exists a positive mean total stress region limited in the very vicinity of the injection well. Meanwhile, there exists a wide region of negative mean total stress locating a little far away from the injection well; this region is expanding toward the injection well with further operation of EGS heat extraction.

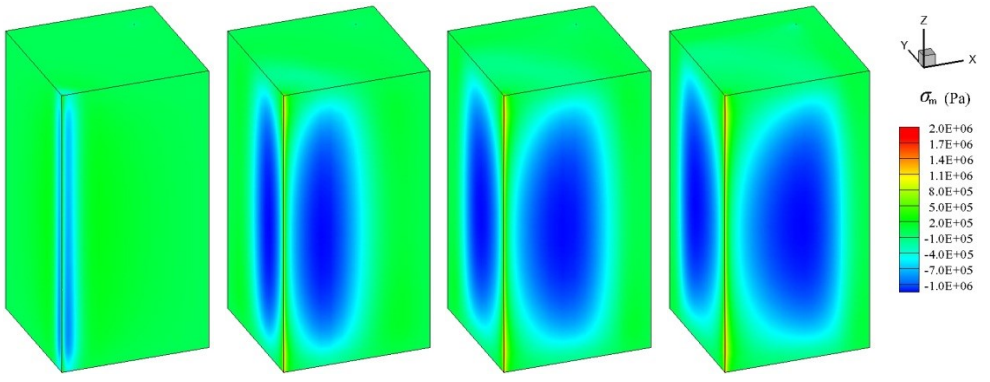

(a) 1 year **(b) 5 years** **(c) 10 years** **(d) 15 years**

Fig. 5: Mean total stress distribution in the heat reservoir

In order to differentiate the thermal and hydraulic contributions to the mechanical process, the poroelastic and thermoelastic stress are broken down from the calculated mean total stress. Fig. 6 compares the poroelastic and thermoelastic stress distribution in the reservoir at 5 years into the EGS operation. It can be seen that the poroelastic stress is compressive and concentrates in the vicinity of the injection well. The maximum compressive stress is induced about the injection well borehole where the pore pressure is the highest. The thermal stresses are tensile in the low temperature region about the injection well. The tensile stresses force the fractures to open and increase the porosity (also permeability) in this region.

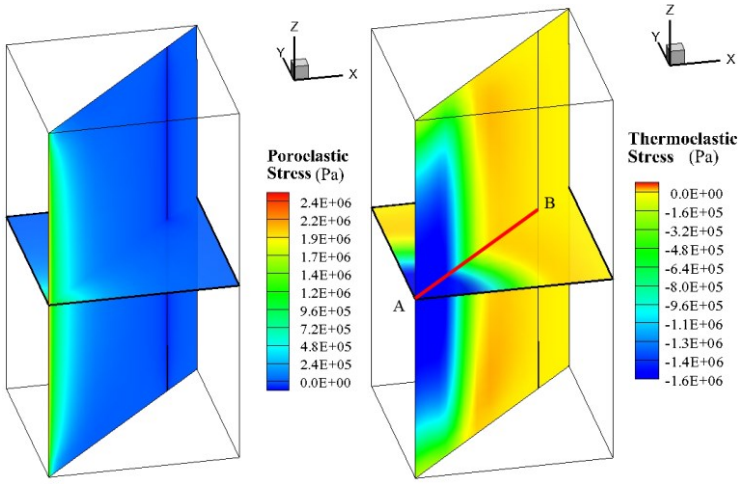

Fig. 6: Distribution of thermo- and poro- elastic stress at 5 years into the EGS operation

To better understand the fluid-rock interactions involved in the processes, the profiles of the thermoelastic stress and the rock–fluid temperature difference at 5 years into the EGS operation are depicted along a selected line AB (position designated in Fig. 6). The rock-fluid temperature difference actually indicates the heat exchange intensity between the rock matrix and fluid in the reservoir as the *ha* is assumed constant in the present work. In terms of the rock-fluid temperature difference, Line AB can be divided into three sub-sections: 1) from 0m to 60m, the temperature difference keeps zero as the rock has been completely cooled down by the fluid; 2) from 60m to 250m, the temperature difference is non-zero positive, meaning that the heat stored in the rock matrix is being mined out by the fluid; 3) from 250m to point B, the temperature difference tends to approach zero as the fluid has been sufficiently heated up by the fluid. It is noteworthy that the variation of the thermoelastic stress also divides line AB into 3 distinct sub-sections, in accordance with the scenario related to the rock-fluid temperature difference profile. Within the subsection from 0m to 60m, the thermoelastic stress maintains at a value around -1.6MPa, which is the cumulative stress caused by prior rock cooling operation. The maximum thermoelastic stress, -1.62MPa, is observed at the point with 60m distance to point A, which is the edge position of apparent heat extraction region. Within the sub-section from 60m to 250m, the magnitude of the thermoelastic stress decreases with the increase of distance to point A. In the last sub-section, from 250m to point B, the thermoelastic stress is around zero.

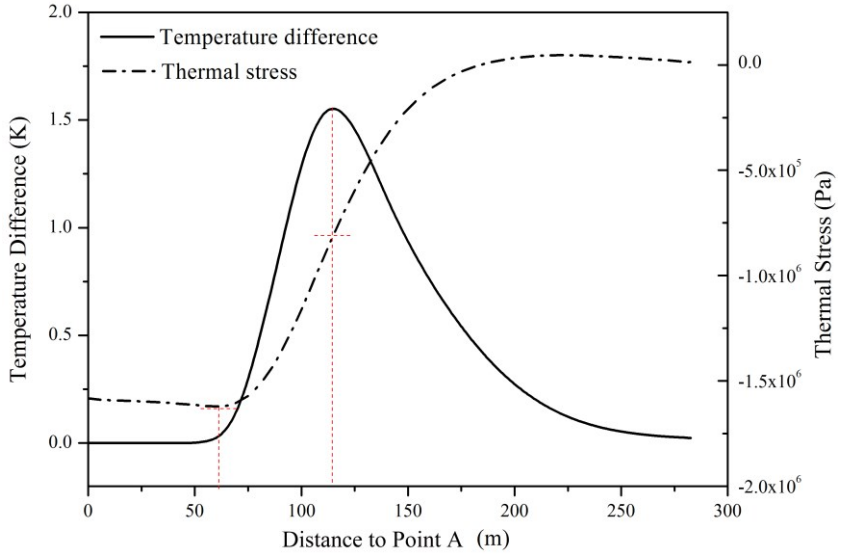

Fig. 7: Profiles of thermoelastic stress and the rock-fluid temperature difference along Line AB at 5 years into the EGS operation

Physically, the rock-fluid temperature difference is the driving force of the heat exchange between the rock matrix and working fluid. With the heat extraction operation goes further, the rock matrix temperature decreases and its volume contracts, leading to tensile stress. The tensile stress is accumulated with the decrease of rock temperature; meanwhile its fastest change position corresponds to the position of maximum rock-fluid temperature difference. Once the temperature of the rock is reduced to the minimum value, i.e. the injection fluid temperature, this tensile stress reaches maximum.

4. SUMMARY AND CONCLUSIONS

We developed a three-dimensional transient model fully coupling the subsurface THM behaviors during EGS heat extraction process. The numerical model was applied to an imaginary quintuplet EGS with cold water injected at a constant temperature and a fixed pressure head. Simulation to the long-term operation of this EGS found that the thermo- and poroelastic stresses altered the

mean total stress state in the reservoir matrix. The thermoelastic effects induced tensile stresses while the poroelastic effects led to compressive stresses. Reasonable results obtained from the simulation indicate the success of THM model development.

ACKNOWLEDGEMENTS

Financial supports received from the CAS "100 talents" Program (FJ), and the China National "863" Project (2012AA052802) are gratefully acknowledged.

REFERENCES

Arairo W., Prunier F., Djeran-Maigre I., et al.: On the use of effective stress in three-dimensional hydro-mechanical coupled model, *Computers and Geotechnics*, **58** (2014) 56-68.

Ghassemi A., Zhou X.: A three-dimensional thermo-poroelastic model for fracture response to injection/extraction in enhanced geothermal systems, *Geothermics*, **40** (2011) 39-49.

Ghassemi A., Tarasovs S., Cheng A.H.D.: A 3-D study of the effects of thermo -mechanical loads on fracture slip in enhanced geothermal reservoirs, *International Journal of Rock Mechanics and Mining Sciences*, **44** (2007) 1132-1148.

Hu L.T., Winterfeld P.H., Fakcharoenphol P., et al.: A novel fully-coupled flow and geomechanics model in enhanced geothermal reservoirs, *Journal of Petroleum Science and Engineering*, **107** (2013) 1-11.

Jeanne P., Rutqvist J., Vasco D., et al.: A 3D hydrogeological and geomechanical model of an enhanced geothermal system at the Geysers, California, *Geothermics*, **51** (2014) 240-252.

Jiang F.M., Luo L., Chen J.L., A novel three-dimensional transient model for subsurface heat exchange in enhanced geothermal systems, *International Communications in Heat and Mass Transfer*, **41** (2013) 57-62.

Jiang F.M., Chen J.L., Huang W.B., et al.: A three-dimensional transient model for EGS subsurface thermo-hydraulic process, *Energy*, (2014) (In press).

Koh J., Roshan H., Rahman S.S.: A numerical study on the long term thermo-poroelastic effects of cold water injection into naturally fractured geothermal reservoirs, *Computers and Geotechnics*, **38** (2011) 669-682.

MIT Report: The future of geothermal energy: impact of enhanced geothermal systems (EGS) on the United States in the 21st century[R]. America: Massachussets of Institute of Technology, 2006.

McDermott C.I., Randriamanjatosoa A.R.L., Tenzer H., et al.: Simulation of heat extraction from crystalline rocks: The influence of coupled processes on differential reservoir cooling, *Geothermics*, **35** (2006) 321-344.

McDermott C.I., Kolditz O.: Geomechanical model for fracture deformation under hydraulic, mechanical and thermal loads, *Hydrogeology Journal*, **14** (2005) 485-498.

Nathenson M.: The dependence of permeability on effective tress from flow tests at hot dry rock reservoirs at Rosemanowes (Cornwall) and Fenton Hill (New Mexico), *Geothermics*, **28** (1999) 315-340.

Rawal C., Ghassemi A.: A reactive thermo-poroelastic analysis of water injection into an enhanced geothermal reservoir, *Geothermics*, **50** (2014) 10-23.

Rutqvist J.: Status of the TOUGH-FLAC simulator and recent applications related to coupled fluid flow and crustal deformations, *Computers & Geosciences*, **37** (2011) 739-750.

Rutqvist J., Wu Y.S., Tsang C.F., et al.: A modeling approach for analysis of coupled multiphase fluid flow, heat transfer, anddeformation in fracturedporous rock, *International Journal of Rock Mechanics & Mining Sciences*, **39** (2002) 429–442.

The International Association for the Properties of Water and Steam. Revised Release on the IAPWS Industrial Formulation 1997 for the Thermodynamic Properties of Water and Steam. Switzerland, 2007.

The International Association for the Properties of Water and Steam. lamda Release on the IAPWS Formulation 2011 for the Thermal Conductivity of Ordinary Water Substance. Czech Republic, 2011.

The International Association for the Properties of Water and Steam. Viscosity Release on the IAPWS Formulation 2008 for the Viscosity of Ordinary Water Substance. Germany, 2008.